

Research article

Integration of bulk RNA sequencing to reveal protein arginine methylation regulators have a good prognostic value in immunotherapy to treat lung adenocarcinoma

Zhiqiang Yang^{a,1}, Lue Li^{a,1}, Jianguo Wei^{b,1}, Hui He^c, Minghui Ma^{d,**},
Yuanyuan Wen^{c,*}

^a Department of Respiratory and Critical Care, Zhoushan Hospital, Wenzhou Medical University, Zhejiang, 316000, China

^b Department of Pathology, The First Affiliated Hospital of Zhengzhou University, Zhengzhou, 450052, China

^c Department of Pathology, Zhoushan Hospital, Wenzhou Medical University, Zhejiang, 316000, China

^d Department of Gastrointestinal Surgery, Maoming People's Hospital, Maoming, Guangdong, 525000, China

ARTICLE INFO

Keywords:

Lung adenocarcinoma
Arginine methylation
Tumor microenvironment
Immunotherapy

ABSTRACT

Background: Given the differential expression and biological functions of protein arginine methylation (PAM) regulators in lung adenocarcinoma (LUAD), it may be of great value in the diagnosis, prognosis, and treatment of LUAD. However, the expression and function of PAM regulators in LUAD and its relationship with prognosis are unclear.

Methods: 8 datasets including 1798 LUAD patients were selected. During the bioinformatic study in LUAD, we performed (i) consensus clustering to identify clusters based on 9 PAM regulators related expression profile data, (ii) to identify hub genes between the 2 clusters, (iii) principal component analysis to construct a PAM.score based on above genes, and (iv) evaluation of the effect of PAM.score on the deconstruction of tumor microenvironment and guidance of immunotherapy.

Results: We identified two different clusters and a robust and clinically practicable prognostic scoring system. Meanwhile, a higher PAM.score subgroup showed poorer prognosis, and was validated by multiple cohorts. Its prognostic effect was validated by ROC (Receiver operating characteristic curve) curve and found to have a relatively good prediction efficacy. High PAM.score group exhibited lower immune score, which associated with an immunosuppressive microenvironment in LUAD. Finally, patients exhibiting a lower PAM.score presented noteworthy therapeutic benefits and clinical advantages.

Conclusion: Our PAM.score model can help clinicians to select personalized therapy for LUAD patients, and PAM.score may act a part in the development of LUAD.

1. Introduction

Lung cancer is considered the leading cause of cancer-related deaths worldwide. Additionally, among the pathological types of lung

* Corresponding author.

** Corresponding author.

E-mail addresses: maminghui@126.com (M. Ma), wenyyy@126.com (Y. Wen).

¹ These authors have contributed equally to this work.

Table 1
Basic information of LUAD cohorts included in this study.

Series accession number	Platform used	Number of patients	Region	Prognosis data
GSE13213 (GPL6480)	Agilent-014,850 Whole Human Genome Microarray	LUAD:117	Japan	Overall survival
GSE31210 (GPL570)	Affymetrix Human Genome U133 Plus 2.0 Array	LUAD:226	Japan	Overall survival
GSE37745 (GPL570)	Affymetrix Human Genome U133 Plus 2.0 Array	LUAD:106	Norway	Overall survival
GSE41271 (GPL6884)	Illumina HumanWG-6 v3.0 expression beadchip	LUAD:184	USA	Overall survival
GSE42127 (GPL6884)	Illumina HumanWG-6 v3.0 expression beadchip	LUAD:133	USA	Overall survival
GSE50081 (GPL570)	Affymetrix Human Genome U133 Plus 2.0 Array	LUAD:127	Canada	Overall survival
GSE72094 (GPL15048)	Rosetta/Merck Human RSTA Custom Affymetrix 2.0 microarray	LUAD:398	USA	Overall survival
TCGA-LUAD	NA	LUAD:507; Normal: 59	NA	Overall survival
IMvigor210	Illumina HiSeq 2000 RNAseq	BLCA:348	USA	Overall survival

LUAD: Lung adenocarcinoma; TCGA: The Cancer Genome Atlas; BLCA: Bladder cancer.

cancer, lung adenocarcinoma (LUAD) is now the dominant type [1]. The development and advancement of LUAD is an intricate and gradual phenomenon entailing several elements, phases, and genetic alterations [2,3]. Cancer immunotherapy, based on the human immune system and using immune regulation to play an anti-tumor role, has shown remarkable clinical effects and provided a new treatment model for tumor patients. However, the clinical response rate is low, and many patients have primary or acquired drug resistance or immune checkpoint inhibitor (ICI)-related side effects [4,5]. Aside from this, in light of the highly metastasis nature of LUAD and its significantly heterogeneous prognosis, we are still unable to fully understand the molecular mechanisms underpinning LUAD progression [6–8]. Therefore, it is important to identify markers that will enable us to stratify patients with LUAD so that better treatments can be applied and prognosis can be predicted more accurately.

The development of LUAD is the result of an interaction between permanent genetic and dynamic epigenetic alterations. Therefore, epigenetic alterations specific to different stages of LUAD can be used to diagnose the disease early and assess the prognosis of patients [9,10]. Numerous publications have reported that protein arginine methylation (PAM) modifications are closely associated with a variety of tumors [11,12]. Protein methyltransferases known as PRMTs function as “writers” by catalyzing arginine methylation. They primarily participate in activating and repressing transcription, pre-mRNA splicing, and responding to DNA damage. PRMTs are a family of enzymes that transfer methyl groups from S-adenosylmethionine (SAM) to the arginine residue ω nitrogen atoms of substrate proteins. Among the nine identified human PRMTs, PRMT1, PRMT2, PRMT3, PRMT4, PRMT6 and PRMT8 are type I, PRMT5 and PRMT9 are type II, and PRMT7 is a type III enzyme [13]. PRMT1 and PRMT5 act as “oncoproteins” in abnormal proliferation of tumor cells [14]. Silencing PRMT5 inhibits lung cancer cell proliferation and clone formation in vitro, and inhibits in vivo growth and tumorigenicity of human lung cancer nude mice in situ transplants [15].

PRMTs can also modulate tumor immunotherapy. Regulatory T cell (Treg) function has recently been found to be associated with arginine methylation. Mice with deletion of PRMT5 in Treg cells also develop severe scurvy-like autoimmunity [16]. Consistent with this, transcriptome analysis of Tregs from PRMT5-deficient mice confirmed that deletion of the FOXP3 target gene was associated with reduced Treg suppressor activity. Mechanistically, pharmacological inhibition of PRMT5 by DS-437 also reduced human Treg functions and inhibited the methylation of FOXP3 [17]. Meanwhile, it was recently found that mouse T-cell deletion of PRMT5 in mice reduced the number of peripheral bloods CD4⁺ and CD8⁺ T cells and thymic NK cells [18].

Bioinformatic analysis of the association of PRMT with bladder and liver cancer has been performed [19,20]. Liu et al. conducted an analysis on hepatocellular carcinoma (HCC) samples, classifying them into three distinct subtypes using PAM regulators. The findings of this research contribute novel perspectives to the investigation of potential therapeutic strategies for managing HCC. Grypari et al. reported that PAM regulators are involved in prostate cancer progression [21]. Here, an PAM.score was constructed. Then, by comparing it with 21 previously published signatures we have further substantiated the clinical applicability and robust prognostic performance of our signature. The established PAM.score effectively stratifies patients and accurately predicts the result of immunotherapy. In brief, our research provides a significant point of reference for attaining timely detection, prognostic assessment, categorized administration, personalized therapy, and enhancing the clinical results of individuals with LUAD.

2. Methods

2.1. Data acquisition

The expression data for LUAD was retrieved by searching the GEO database using the following keywords: “lung adenocarcinoma”, “LUAD”, and “lung cancer”. GSE13213 [22], GSE31210 [23], GSE37745 [24], GSE41271 [25], GSE42127 [26], GSE50081 [27], and GSE72094 [28] were selected and downloaded. 117 for GSE13213, 226 for GSE31210, 106 for GSE37745, 184 for GSE41271, 133 for GSE42127, 127 for GSE50081, and 398 for GSE72094. We also adopted from TCGA public database (LUAD:507; normal: 59). A total of 1798 LUAD samples were selected. Additionally, an immunotherapy dataset was from IMvigor210 [29] (Table 1).

2.2. Data preprocessing

The expression value of each sample from TCGA was converted from fragments per kilobase million (FPKM) to transcripts per million (TPM) for subsequent analysis [30]. Quantile normalization and background correction were performed on GEO data using the

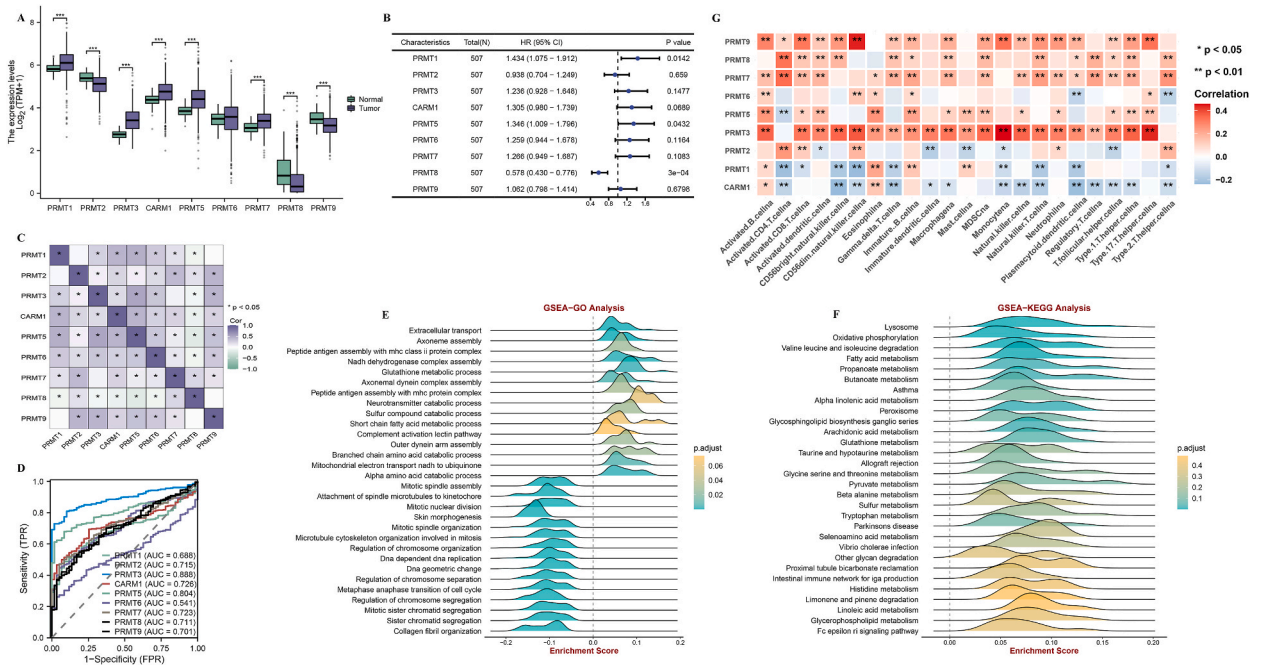


Fig. 1. mRNA expression levels and prognostic value of 9 PAM regulators in LUAD in TCGA-LUAD. (A) The illustration shows the expression distribution of 9 PAM regulators between tumor and normal. (B) Univariate Cox regression analysis of 9 PAM regulators and overall survival in TCGA-LUAD. (C) Correlation heat map of 9 PAM regulators. (D) ROC analysis showed the diagnostic performance of 9 PAM regulators in TCGA-LUAD. (E) GSEA-GO showed that 9 PAM regulators related signaling pathways in LUAD. (F) GSEA-KEGG identified 9 PAM regulators related signaling pathways in LUAD. (G) 9 PAM regulators expression are related to immune in LUAD. (*P < 0.05; **P < 0.01; ***P < 0.001).

“affy” package in R, utilizing the Robust Multi-array Average algorithm [31].

2.3. Molecular subtyping of 9 PAM regulators

To further investigate the assignment of PAM regulators in LUAD, we applied the PAM regulators identified in the co-expression analysis to converge LUAD samples using non-negative matrix factorization. We used the “brunet” criterion with nrun set to 100, and the figure of clusters (k) was assigned from 2 to 10. We determined the mean profile breadth of the ordinary membership matrix using the R package “NMF”. By applying this algorithm, we separated the examples into different molecular sub-types on account of the representative of prognostic-related PAM regulators [32]. Then, we applied the “limma” package to discover DEG between 2 clusters [33].

2.4. Gene enrichment analysis

To identify the potential biological roles and pathways, we applied Gene Ontology (GO) categories and Kyoto Encyclopedia of Genes and Genomes (KEGG) enrichment analyses via the R package “clusterProfiler” [34].

2.5. Procedure for generating score model

To compare the predictive value of PAM.score with other signatures, we summarized 21 published signatures of LUAD (Supplementary Table 1). We use the same methodology as in this paper to compare whether the PAM.score has advantage of predictive value of other signatures. Following is the procedure for generating score model:

- The patients were classified into several clusters for deeper analysis by adopting unsupervised clustering method based on the expression of PAM.
- DEGs analysis and univariate Cox regression analysis were applied to identified signatures between clusters.
- We then conducted principal component analysis (PCA) based on the expression of signatures between clusters.
- The Score of each sample was calculated by

$$\text{Score} = \sum(PC1_i + PC2_i),$$

where “i” represents the gene expression level of related gene expression. The code implementing the score method has been deposited

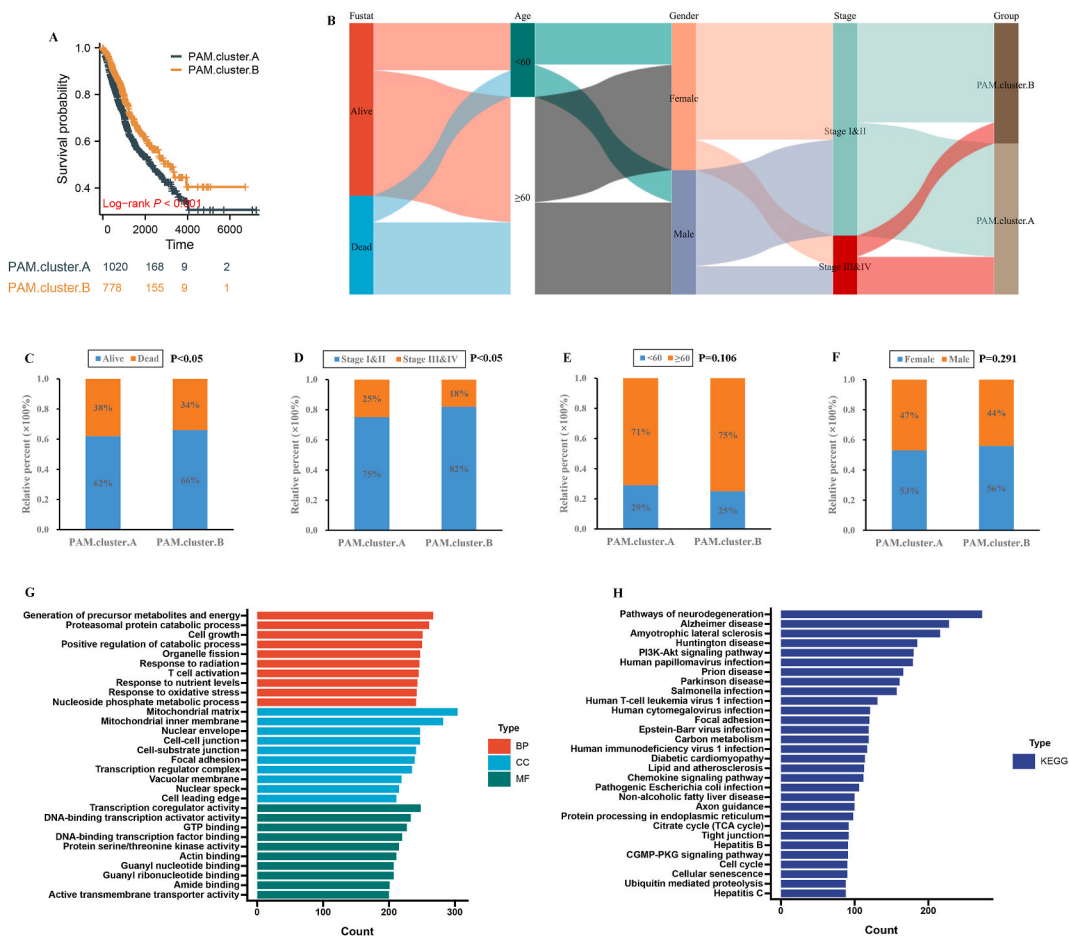


Fig. 2. Molecular classification based on 9 PAM regulators expression. (A) Kaplan-Meier curve showed a significant overall survival difference between the 2 PAM.clusters. (B) Alluvial diagram showing the relationship between the 2 PAM.clusters and clinical characteristics. (C–F) The relationship between the 2 PAM.clusters and patients' status, patients' stage, patients' age, and patients' gender. (G) GO enrichment analysis, (H) KEGG enrichment analysis for the different expression genes between the 2 PAM.clusters (BP means Biological Process; CC means Cell Component; MF means Molecular Function).

in git hub (<https://github.com/wen571/PAMscore>). Based on the median value of the score, patients were divided into high and low score subgroups. The code implementing the PAM.score method has been deposited in git hub (<https://github.com/wen571/PAMscore>).

2.6. Prediction immunotherapy responses

The tumor immune dysfunction and exclusion (TIDE) was used to predict the responses to immunotherapy. The TIDE is a method of assessing immune evasion by taking into account the expression characteristics of both T-cell exclusion and T-cell dysfunction. Our investigation aimed to evaluate the influence of risk score prediction models on clinical outcomes through the application of TIDE [35].

2.7. GSEA

Enrichment analysis was performed by the cluster profile package. We used the GSEA program to calculate single-sample gene set enrichment. To control the FDR, the p values were obtained after 1000 permutations and were adjusted for multiple testing [36].

2.8. Evaluation of TME in LUAD

The infiltration abundance among patients in high and low PAM.score groups was calculated using the ssGSEA algorithm [37]. Based on the median value of the ESTIMATE score, patients were divided into high and low score subgroups. Independent predictive value of PAM.score and ESTIMATE score features were verified using univariate and multivariate Cox regression analyses by the

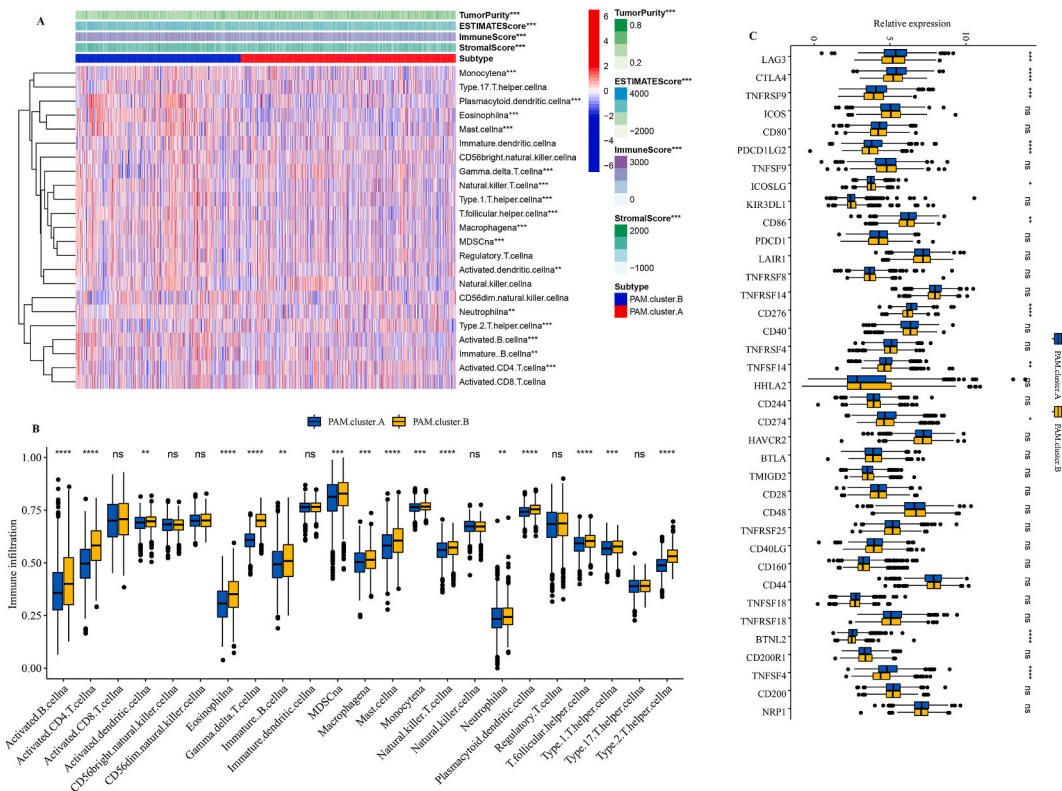


Fig. 3. TME between the 2 PAM.cluster. (A) The relationship between the 2 PAM.clusters and TME. Red is cluster.A and blue is cluster.B. (B) The abundance of each TME infiltrating cell in 2 PAM.clusters. Blue is cluster.A and yellow is cluster.B. (C) The abundance of immune checkpoint condition in 2 PAM.clusters. (cluster.B vs cluster.A. *P < 0.05; **P < 0.01; ***P < 0.001; ****P < 0.0001).

“survival” R package [38].

2.9. Single-cell RNA sequencing analysis

GSE149655 containing 2 normal and 2 LUAD samples, were downloaded from GEO database. First, the data was imported into R to generate a Gene-barcode matrix, cells with a gene number (nFeature_RNA) between 500 and 2000 are retained, and cells with mitochondrial genes greater than 25% are filtered. Then “Seurat” was used for log normalization of the data, “FindVariableFeatures” was used to find 2000 hypervariable genes, followed by data normalization, and PCA linear dimensionality reduction was performed on the normalized data, resulting in 12,554 cells. At the same time, PCA downscaling was performed by run PCA to find anchor points (set Resolution = 0.1), perform TSNE downscaling analysis by run TSNE function, and show the distribution of different samples by TSNE plot.

2.10. Statistical analysis

The data was analyzed by R version 3.6.3 software. Wilcoxon test was used for comparison between two groups. Spearman analysis was performed to assess the correlation between PAM regulators expression levels and immune cell infiltration levels. Kaplan–Meier method was used to estimate overall survival (OS). Differences in survival rates were compared with log-rank tests. P < 0.05 was considered statistically significant.

3. Results

3.1. mRNA expression levels and prognostic value of 9 PAM regulators in LUAD

To clarify the expression of 9 PAM regulators in LUAD, RNA sequencing data in TCGA was examined. The differential 9 PAM regulators expression patterns in LUAD and normal tissues are shown in Fig. 1A. The expression of PRMT1, PRMT3, CARM1, PRMT5, PRMT7 were significantly higher in LUAD than in normal tissues. The expression of PRMT2, PRMT8, PRMT9 were significantly lower in LUAD than in normal tissues. Next, we analyzed the prognostic impact of 9 PAM regulators expression on LUAD patients in the TCGA

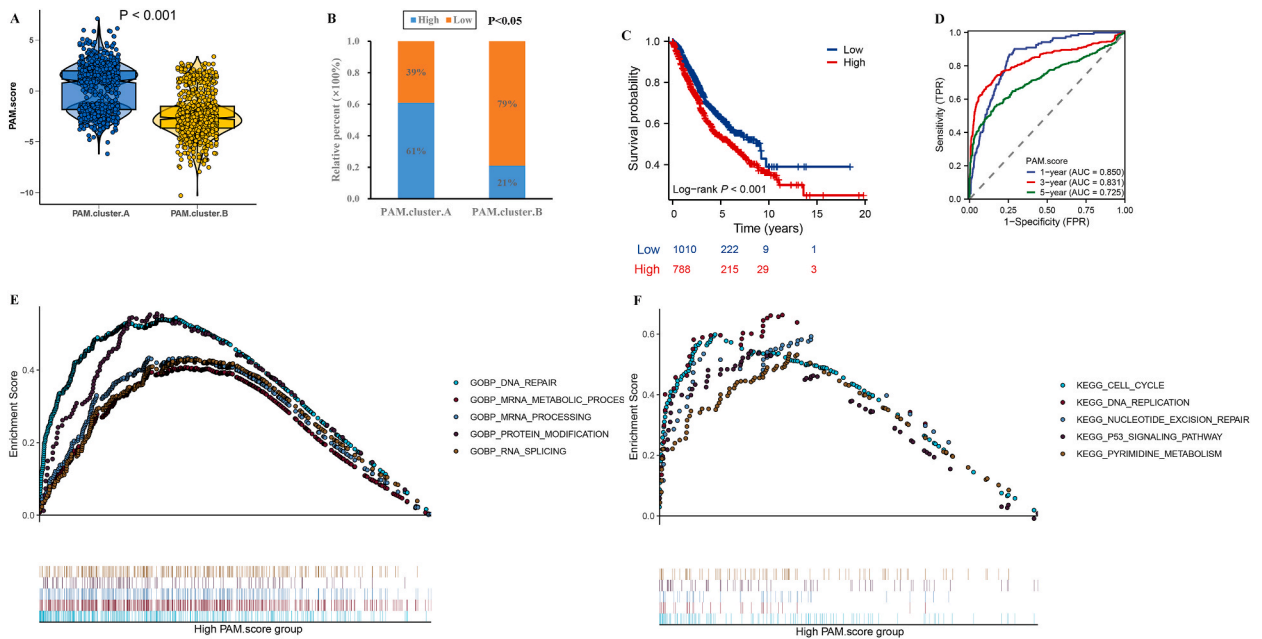


Fig. 4. PAM.score model was constructed based on 9 PAM regulators. (A) Differences in PAM.score among 2 PAM.clusters. (B) The number of high and low PAM.score patients in 2 PAM.clusters groups. (C) Kaplan-Meier curve showed a significant overall survival difference between high and low PAM.score groups. (D) The prognostic value of PAM.score. (E) GSEA GO identified high PAM.score groups related signaling pathways in LUAD. (F) GSEA KEGG identified high PAM.score groups related signaling pathways in LUAD. Each small cell below the horizontal coordinate represents the number of genes enriched in the pathway.

database using a univariate COX risk proportional regression model. For overall survival (OS), higher PRMT1 and PRMT5 expression was associated with poorer survival in LUAD patients. Whereas, lower expression of PRMT8 in LUAD patients was associated with a survival disadvantage (Fig. 1B). Meanwhile, through a comprehensive examination, we conducted an in-depth analysis of the interconnections existing among these 9 regulators of PAM. Intriguingly, our findings provide compelling evidence that these entities exhibit a remarkably close association (Fig. 1C). Among the 9 PAM regulators, PRMT3 and PRMT5 have a higher AUC value, indicating their prognostic value for LUAD (Fig. 1D).

3.2. 9 PAM regulators are related to tumor microenvironment in LUAD

First, we found that 9 PAM regulators were enriched for cell cycle and immune-related terms, such as peptide antigen assembly with MHC class ii protein complex, peptide antigen assembly with MHC protein complex (Fig. 1E and F). Next, we identified the relationship between 9 PAM regulators expression and immune cells infiltration based on the 'ssGSEA' algorithm. The results suggest that the expression level of 9 PAM regulators generally showed a significant correlation with the infiltration level in LUAD (Fig. 1G).

3.3. Molecular classification based on 9 PAM regulators expression

The NMF algorithm was made use of clustering the samples in accordance with the utterance standard of foreknowledge. The first-rank number of clusters was 2 (PAM.cluster.A and PAM.cluster.B). To better explore the prognosis features of these clusters, we adopted Kaplan-Meier analysis. We figured out that the OS time of the PAM.cluster.A had poor prognosis compared with PAM.cluster.B (Fig. 2A). The results also suggest that PAM.cluster.A had higher dead and stage III&IV patients compared with PAM.cluster.B (Fig. 2B–F). In PAM.cluster.A, a significant increase in the expression levels of PRMT1, PRMT3, PRMT5, PRMT6, PRMT7, and PRMT9 was observed compared to those in PAM.cluster.B, however, a significant decrease in the expression levels of PRMT8 was observed compared to those in PAM.cluster.B (Supplementary Fig. 2).

Next, differentially expressed genes between the 2 PAM.clusters were detected (Supplementary Table 2). Then we applied GO and KEGG, and the different genes between the 2 PAM.cluster was remarkably enriched immune-related pathways (T cell activation, human T-cell leukemia virus 1 infection, human immunodeficiency virus 1 infection) and cancer-related pathways (cell cycle) (Fig. 2G and H, Supplementary Tables 3 and 4).

3.4. TME between the 2 PAM.cluster

The immune marks and immune infiltration between the molecular subcategories were made comparison using ssGSEA and

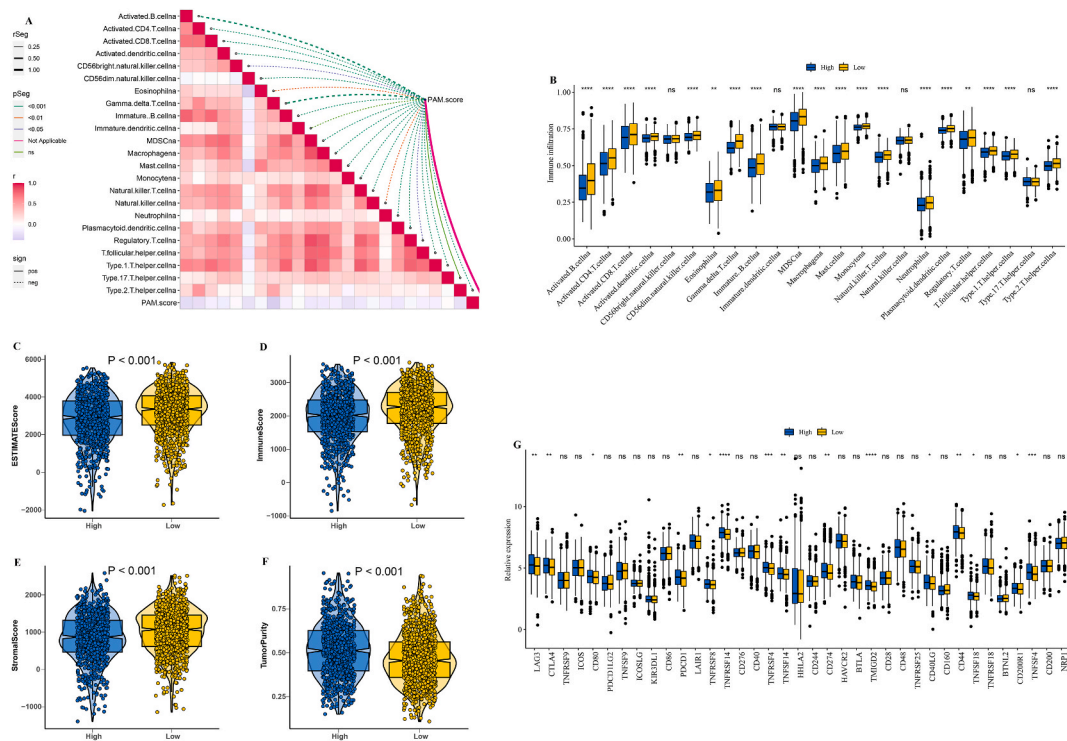


Fig. 5. TME between the high and low PAM.score groups. (A) The correlation between PAM.score and different immune cells. (B) The abundance of each TME infiltrating cell in high and low PAM.score groups. (C–F) The ESTIMATE score, stromal score, immune score, and tumor immunity levels in high and low PAM.score groups. (G) The expression of immune checkpoint condition between high and low PAM.score groups. The solid line represents the positive correlation and the dotted line represents the negative correlation. The depth of the color represents the size of the correlation, the darker the color, the greater the correlation. (High vs low * $P < 0.05$; ** $P < 0.01$; *** $P < 0.001$; **** $P < 0.0001$).

ESTIMATE. Significant variations existed in the relative proportions of immune cell populations when comparing the 2 groups (Fig. 3A and B, Supplementary Table 5). Additionally, the PAM.cluster.A group had lower immune score, stromal score, estimate score, and higher tumor purity in comparison to the PAM.cluster.B group (Supplementary Fig. 3 A–D, Supplementary Table 6). Moreover, in comparison to PAM.cluster.B group, check-points exhibited noticeable elevation in the PAM.cluster.A group (Fig. 3C–Supplementary Table 7).

3.5. PAM.score model was constructed based on 9 PAM regulators

In order to better understand the PAM regulators, we calculated the PAM.score of each sample and normalized it. According to the PAM.score distribution, the high and low PAM.score subgroups had significant differences (Supplementary Table 8). According to the findings, it was observed that the RPMscore was comparatively lower in PAM.cluster.B when compared to PAM.cluster.A (Fig. 4A). Additionally, the group belonging to PAM.cluster.A presented a significantly higher number of patients with a high PAM.score (Fig. 4B). Next, K-M survival analysis demonstrated that individuals belonging to high PAM.score group exhibited a significantly decreased OS when compared low PAM.score (Fig. 4C). In addition, we conducted ROC curve analysis to evaluate the performance of the PAM.score, the AUC was 0.850 for 1-year, 0.831 for 3-year and 0.725 for 5-year (Fig. 4D). We also found the expression of PRMT1, PRMT2, PRMT3, PRMT5, PRMT6, PRMT7, PRMT9 were significantly higher in high PAM.score group than in low PAM.score group. A significant decrease in the expression levels of PRMT8 was observed in high PAM.score compared to those in low PAM.score (Supplementary Fig. 4). GSEA showed that mRNA-related pathways (mRNA processing, mRNA metabolic process, RNA splicing) and tumor-related pathways (DNA repair, cell cycle, P53 signaling pathway) were enriched in the high PAM.score group (Fig. 4E and F). These results suggested that high PAM.score may have a significant impact in tumor development.

3.6. TME between the high and low PAM.score groups

Using multiple immune algorithms, we examined the immune landscape for the high/low PAM.score groups to investigate the underlying mechanism between the PAM.score and immunity (Fig. 5A, Supplementary Table 9). Significant variations existed in the relative proportions of immune cell populations when comparing the low and high PAM.score groups. As the PAM.score increased, the overall level of immune infiltration decreased (Fig. 5B). TME was also evaluated using the ESTIMATE software. It was observed that

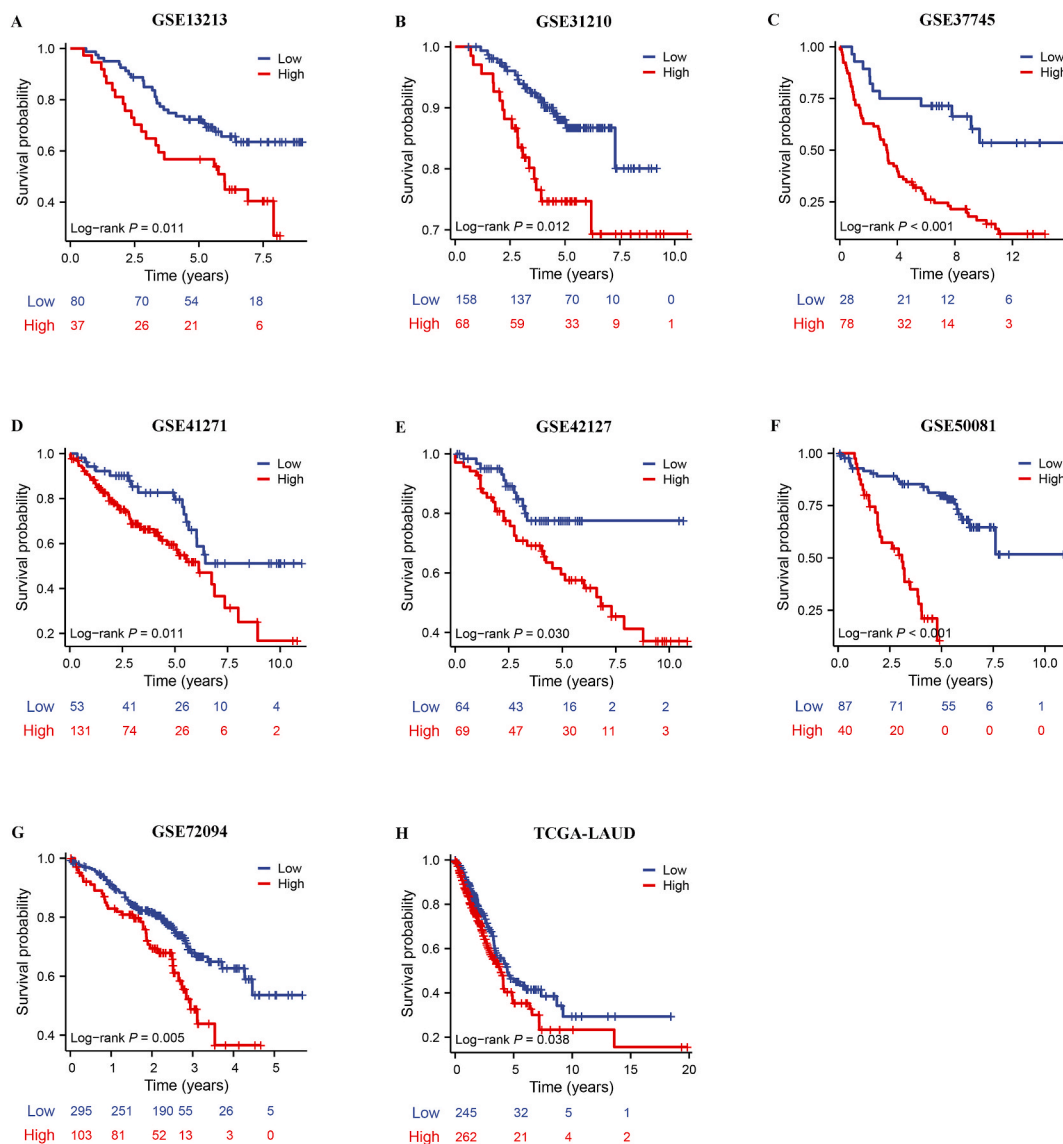


Fig. 6. External validation of PAM.score. (A–H) Kaplan-Meier curve showed a significant overall survival difference between high and low PAM.score groups in GSE13213, GSE31210, GSE37745, GSE41271, GSE42127, GSE50081, GSE72094, and TCGA dataset.

the high PAM.score group exhibited lower immune score, stromal score, estimate score, and higher tumor purity in comparison to the low PAM.score group (Fig. 5C–F, Supplementary Table 10). Additionally, compared with high PAM.score group, check-points were downregulated in low PAM.score group (Fig. 5G).

3.7. PAM.score is a robust prognosis factor in LUAD

Next, the results of the K-M survival analysis demonstrated that individuals belonging to the high PAM.score group exhibited a significantly decreased OS when compared to those in the low PAM.score group within both all cohorts (GSE13213, GSE31210, GSE37745, GSE41271, GSE42127, GSE50081, GSE72094, and TCGA dataset) (Fig. 6A–H). Next, after adjust ESTIMATEScore, immuneScore, stromalScore, and tumorPurity, the LUAD prognosis can be predicted by utilizing the PAM.score as an independent factor (Fig. 7A).

3.8. Comparisons between PAM.score and 21 published signatures in LUAD

Next, we extensively extracted published signatures in order to evaluate and contrast the effectiveness of the PAM.score in comparison to other signatures associated with LUAD. Ultimately, 21 signatures were included in the subsequently comparisons. It is

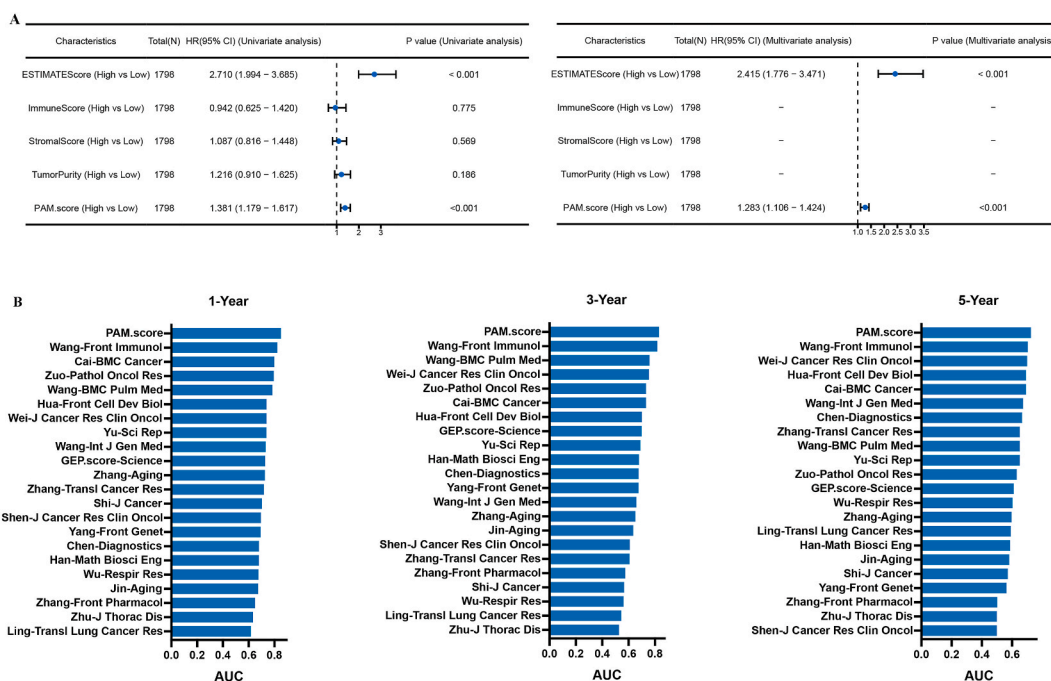


Fig. 7. Evaluation of the PAM.score. (A) Univariate and multivariate Cox regression analysis of PAM.score in the LUAD. (B) The performance of PAM.score was compared with 21 published signatures.

important to highlight that PAM.score outperforms nearly all models in every dataset (Fig. 7B).

3.9. Immunotherapy response targeting PAM.score

Since the development of the PAM.score is based on immune-related patterns and the significant differences in immune characteristics between the two groups, we speculated that the sensitivity of LUAD patients with high/low PAM.score to immunotherapy will also be different. With the aid of immune response testing algorithms and features, we verified the predictive potential of the PAM.score for immunotherapy response. The results suggested that patients in the low PAM.score group exhibited a higher immune response rate (Fig. 8A–C, Supplementary Table 11).

Next, PAM.score model was constructed based on 9 PAM regulators in IMvigor210 cohort, and revealed that significance between the high/low PAM.score (Supplementary Table 12). The results of the K-M survival analysis demonstrated that individuals belonging to the high PAM.score group exhibited a significantly decreased OS when compared to those in the low PAM.score group (Fig. 8D). In addition, we conducted ROC curve analysis to evaluate the performance of the PAM.score, the AUC was 0.828 for 1-year, 0.779 for 3-year and 0.814 for 5-year (Fig. 8E). Moreover, the PAM.score exhibited higher in SD/PD group in IMvigor cohort (Fig. 8F and G). Moreover, in the high PAM.score group, the proportion of CR/PR patients was notably lower compared to the low PAM.score group (17% vs. 30%) (Fig. 8H).

3.10. Single-cell RNA sequencing analysis the PAM.score in LUAD

To assess the distribution of PAM.score in LUAD on cell level, we analyzed 12,554 cells derived from 2 normal and 2 LUAD samples in GSE149655. Using dimensional reduction and clustering analysis methods, we effectively identified 8 unique cellular types and 12 clusters of cells within the LUAD tissues (Fig. 9A and B). In addition to B cells and macrophages, monocytes cluster is also more abundant in LUAD than normal tissue. Notably, Fig. 9C illustrates the top 5 markers genes in these eight cell types. KEGG was performed on the cluster of eight cell types, we found that eight cell types enriched cells were mainly enriched in immune-related pathways (Fig. 9D). We also found RMT1 was mainly distributed in macrophage, PRMT5 was mainly distributed in B cell, PRMT8 was mainly distributed in epithelial cells (Fig. 10A). We also found that the expression of PRMT1, CARM1, and PRMT5 were significantly higher in LUAD than in normal cells. The expression of PRMT8, PRMT9 were significantly lower in LUAD than in normal cells (Fig. 10B). Finally, we also revealed that PAM.score of tumor cells were considerably higher than those of normal cells (Fig. 10C).

4. Discussion

LUAD is one of the most fatal malignancies in the world. Moreover, due to the existence of tumor heterogeneity and variations in

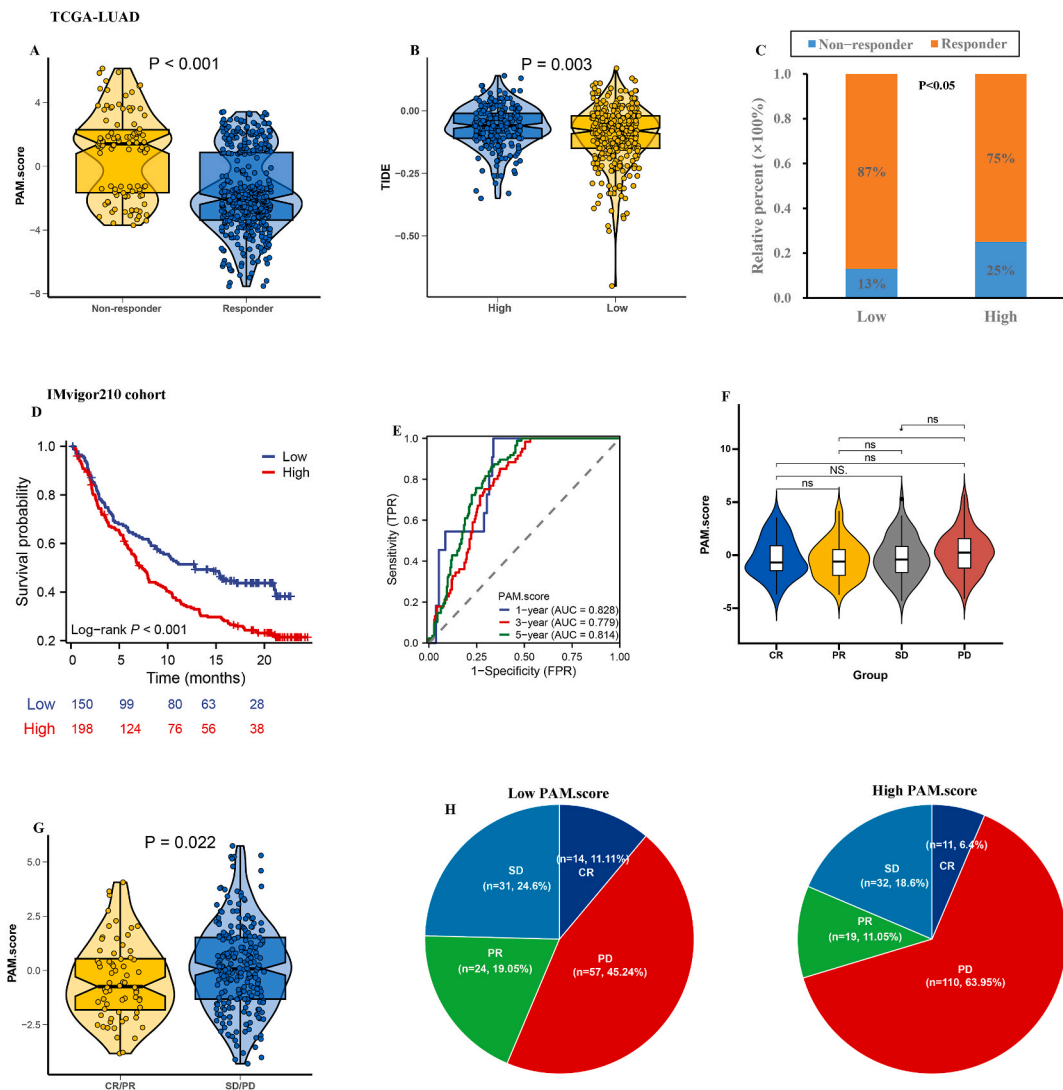


Fig. 8. PAM.score in the role of anti-PD-1/L1 immunotherapy. (A) Differences in PAM.score among non-response and response groups. (B) Differences in TIDE among high and low PAM.score groups. (C) The proportion of non-response and response patients in low and high PAM.score groups. (D) Kaplan-Meier curve showed a significant overall survival difference between low and high PAM.score groups in IMvigor210 cohort. (E) The prognostic value of PAM.score in IMvigor210 cohort. (F) Distribution of PAM.score in CR, PR, SD, and PD groups. (G) Differences in PAM.score among CR/PR and SD/PD groups. (H) The number of CR, PR, PD, and SD patients in high and low PAM.score groups. (*P < 0.05; **P < 0.01; ***P < 0.001; ****P < 0.0001).

clinical outcomes among patients staged simultaneously, the conventional practice of clinical staging imparts restricted outcomes in terms of risk assessment and prognosis management for patients sharing the same stage. The urgent need arises from the aforementioned reasons to establish reliable prognostic biomarkers. These biomarkers can be identified through the usage of optimal algorithms in order to categorize patients with LUAD and determine their eligibility for immunotherapy, thereby benefiting them. Previous literature has reported that PAM regulators especially the PRMT5 is closely related to tumor development, but no comprehensive analysis of PAM regulators has been conducted from a holistic perspective in LUAD. This study aimed to systematically investigate the expression pattern, prognostic value, and potential function of PAM regulators in LUAD.

We first observed that PRMT1, PRMT3, CARM1, PRMT5, PRMT7 were generally highly expressed in LUAD, while there was a significant decrease in PRMT2, PRMT8, PRMT9 compared to normal tissues. Survival analysis revealed upregulated expression of PRMT1 and PRMT5 were associated with poorer OS in LUAD, and downregulated expression of PRMT8 had a worse survival in LUAD. Meanwhile, PRMT1, PRMT5, and PRMT8 also have high diagnostic value for LUAD. In summary, PRMT1, PRMT5, and PRMT8 can be used as a prognostic marker in LUAD.

Our analysis findings closely align with existing literature, which states that PAM regulators show variability in expression levels and exhibit diverse biological functions across various tumor types. Moreover, they might potentially fulfill distinct roles. For example,

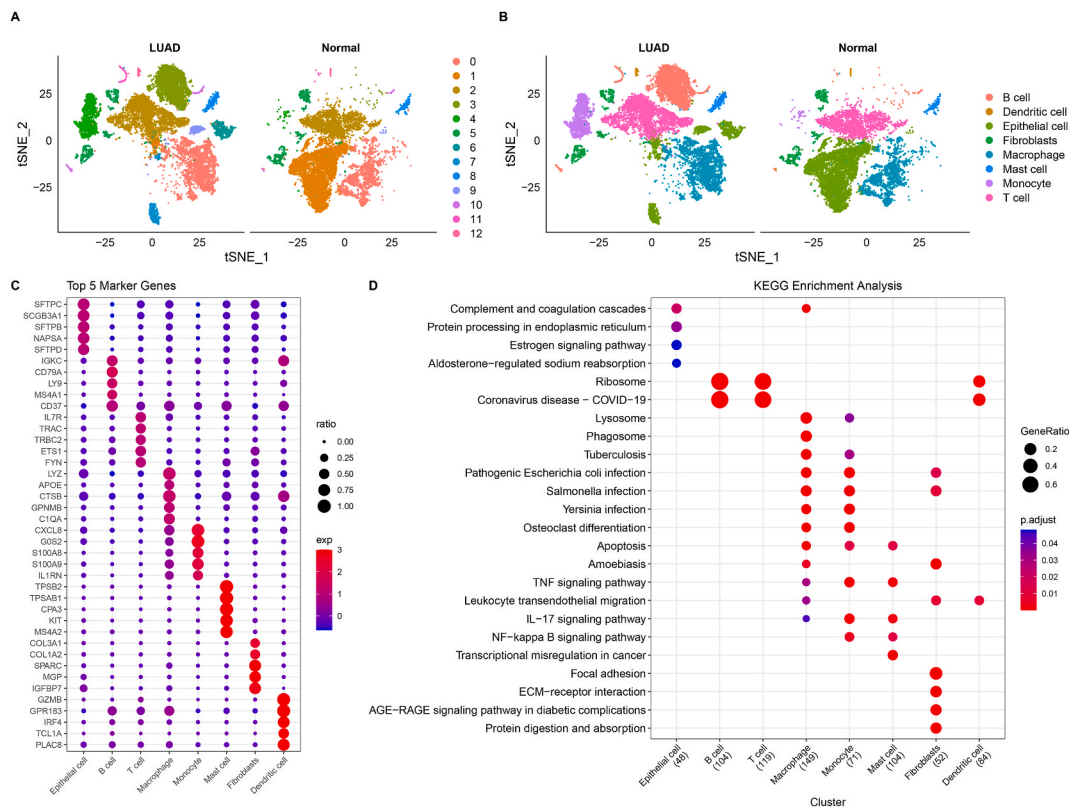


Fig. 9. Sc-RNA sequencing analysis in GSE149655. (A) The clusters of GSE149655 based on tSNE. (B) The annotated cell types of GSE149655 based on tSNE. (C) The top 5 markers genes in these eight cell types. (D) KEGG revealed the enrichment pathways of eight cell types.

overexpression of PRMT1 promotes epithelial mesenchymal transition through H4R3me2a-mediated regulation of the ZEB1 promoter [39], whereas PRMT1 and the lysine demethylase KDM4C are co-recruited to the Hoxa9 promoter via MOZTIF2 and MLL fusion proteins to promote H4R3me2a and H3K9 demethylation, respectively [40]. Thus, drugs targeting PRMT1 may act by inhibiting aberrant epigenetics in tumor cells. PRMT5 can also drive or repress gene transcription depending on the modification of histone tail residues, thus regulating gene expression at the epigenetic level to regulate gene expression [41]. PRMT8 also contributes to the maintenance of pluripotency in human embryonic stem cells through its ability to induce the expression of SOX2 [42].

In this analysis, we identified 2 clusters, cluster.A may be associated with worse prognosis in LUAD patients. To delve deeper, we further carried out enrichment analyses for DEGs between 2 clusters. We have identified a notable distinction in immune-related assessment and clinical pathological characteristics for immune subtype categorization. These findings serve as evidence that the classification of LUAD can be enhanced through the differentiation of clusters based on PAM regulators. This innovative approach offers a new pathway in immune subtype classification. To better serve the clinic, we constructed a PAM.score based on DEGs and prognostic genes between 2 clusters offering valuable direction for the therapy of LUAD. Kaplan-Meier survival curve analysis indicated the OS rate was greatly higher in suffers with a high-risk mark than those with a low-risk mark, suggesting the score is related to patient outcome. Risk scores can significantly distinguish between the clinical features of different suffers. The clinical characteristics of suffers in the high and low-risk groups were significantly different, with dead patients significantly increasing as scores increased. These results suggest that the clinical characteristics of suffers in the high-risk group are greatly worse than those in the low-risk group. The model can also make good predictions on adverse clinical traits. Furthermore, multivariate Cox regression analysis revealed this pattern was an independent risk element for LUAD, making it a valid biomarker for LUAD prognosis. In addition, the outcomes of GSEA exposed the high-risk group suffers exhibited an enrichment in tumor-related pathways. Obviously, prior research has suggested these pathways take a great part in tumor proliferation, migration, invasion, and metastasis. These findings offer a novel orientation for exploring the feasible molecular system of LUAD.

Immunotherapy has made it possible to treat LUAD in a new manner. In spite of this, immunotherapy is only effective for a small number of patients. The Checkmate-017 and Checkmate-057 trials first introduced nivolumab to the second-line treatment of non-small cell lung cancer, and both clinical trials succeeded in pitting nivolumab against the standard second-line chemotherapy regimen docetaxel, thus establishing immunotherapy as a second-line treatment for non-small cell lung cancer [43,44]. Immunotherapy has shown great potential, but there are still some problems that plague clinicians. The first is how to select biomarkers to effectively predict the efficacy of checkpoint inhibitors. The KEYNOTE-024 study, which was screened in a highly selected population (PD-L1 \geq 50%), while Checkmate-026 did not meet the endpoints [45,46]. In this analysis, the low PAM.score group identified 8%

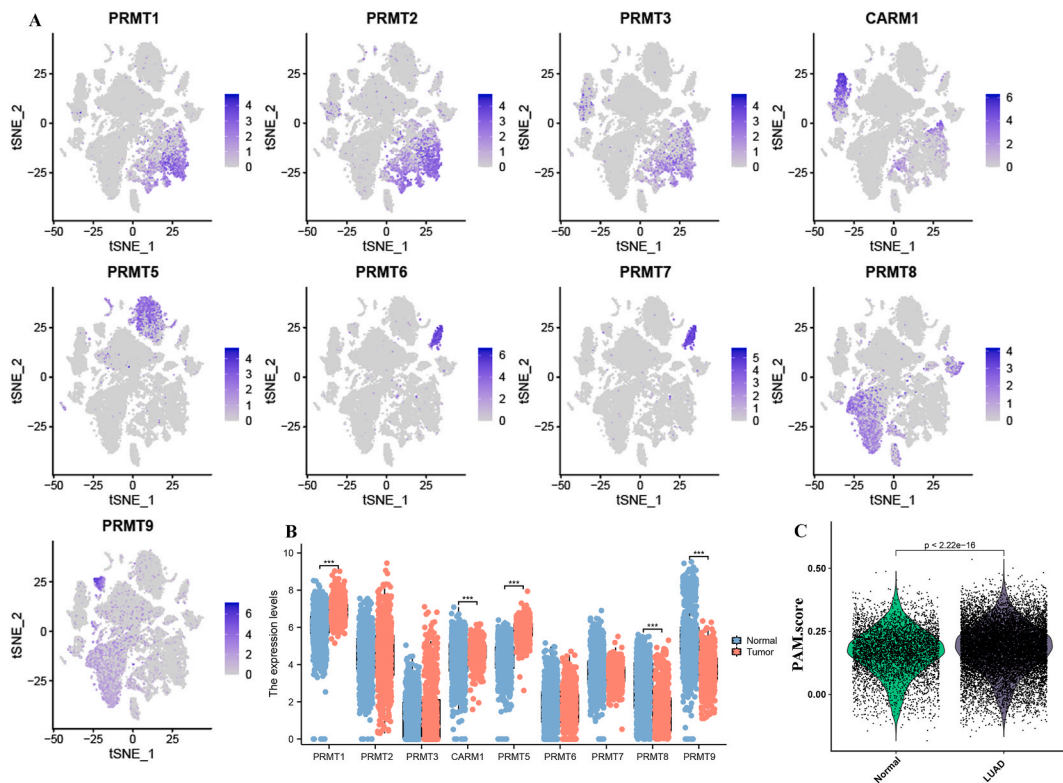


Fig. 10. Sc-RNA sequencing analysis reveal the PAM.score on single cell level. (A) The distribution of 9 PAM regulators in eight cell types. (B) The different of 9 PAM regulators between normal cells and LUAD cells. (C) The different of PAM.score between normal cells and LUAD cells.

more patients effective for immunotherapy than the high PAM.score group, demonstrating its superiority among biomarkers.

Although we have explored this relationship to some extent and built and acknowledged an ominous pattern on the basis of data from various datasets, there are still some limitations. This study only verified the PAM.score in LUAD in vitro, which was not validated using in vivo assays. It is, therefore, necessary to elucidate the molecular mechanisms of PAM.score at the cellular and molecular levels, which will be more helpful in elucidating the role of PAM.score in different cancers. Besides, the connection among PAM.score, infiltration of immune cells in tumors, and patient survival was evaluated. The findings indicated a significant association between PAM.score, tumor immune cell infiltration, and patient survival. Nevertheless, our study did not establish a direct link between PAM.score and patient survival via immune cell infiltration. To obtain conclusive outcomes, forthcoming prospective investigations should focus on exploring the association of PAM.score and immune cell infiltration in the LUAD population. Finally, in this paper, we did not analyze the effect of EGFR or K-ras mutations on the model due to the small sample information of EGFR or K-ras.

5. Conclusion

To recapitulate, we created a strong identifier termed PAM.score using the fields of bioinformatics to evaluate the forecast, classification of risk, and immunotherapy reaction in relation to LUAD. In light of our study and previous literature on PAM, it is an emerging and promising area for further investigation. We hope that future research will continue to explore its potential implications in the field of oncology.

Ethics approval and consent to participate

Not applicable.

Consent for publication

Not applicable.

Funding

Zhejiang Medical and Health Science and Technology Project (2019KY739); Zhejiang Provincial Administration of Traditional

Chinese Medicine (2021ZB349). This study was also supported by High-level Hospital Construction Research Project of Maoming People's Hospital.

Data availability

The data that support the findings of this study are openly available in [TCGA] at [<https://portal.gdc.cancer.gov/repository>], reference number [TCGA-LUAD], and the data that support the findings of this study are openly available in [GEO] at [<https://www.ncbi.nlm.nih.gov/gds>], reference number [GSE13213, GSE31210, GSE37745, GSE41271, GSE42127, GSE50081, GSE72094, and GSE149655].

CRedit authorship contribution statement

Zhiqiang Yang: Validation, Formal analysis, Data curation. **Lue Li:** Software, Data curation. **Jianguo Wei:** Validation, Data curation. **Hui He:** Software, Formal analysis. **Minghui Ma:** Writing – original draft, Validation. **Yuanyuan Wen:** Writing – review & editing, Writing – original draft.

Declaration of competing interest

The authors declare that they have no known competing financial interests or personal relationships that could have appeared to influence the work reported in this paper.

Acknowledgments

None.

Appendix A. Supplementary data

Supplementary data to this article can be found online at <https://doi.org/10.1016/j.heliyon.2024.e24816>.

References

- [1] R.L. Siegel, K.D. Miller, N.S. Wagle, A. Jemal, Cancer statistics, 2023, *CA A Cancer J. Clin.* 73 (2023) 17–48.
- [2] K.D. Miller, L. Nogueira, T. Devasia, A.B. Mariotto, K.R. Yabroff, A. Jemal, J. Kramer, R.L. Siegel, Cancer treatment and survivorship statistics, 2022, *CA A Cancer J. Clin.* 72 (2022) 409–436.
- [3] F.R. Hirsch, G.V. Scagliotti, J.L. Mulshine, R. Kwon, W.J. Curran Jr., Y.L. Wu, L. Paz-Ares, Lung cancer: current therapies and new targeted treatments, *Lancet (London, England)* 389 (2017) 299–311.
- [4] C. Genova, C. Dellepiane, P. Carrega, S. Sommariva, G. Ferlazzo, P. Pronzato, R. Gangemi, G. Filaci, S. Coco, M. Croce, Therapeutic implications of tumor microenvironment in lung cancer: focus on immune checkpoint blockade, *Front. Immunol.* 12 (2021) 799455.
- [5] Y. Wang, R. Chen, Y. Wa, S. Ding, Y. Yang, J. Liao, L. Tong, G. Xiao, Tumor immune microenvironment and immunotherapy in brain metastasis from non-small cell lung cancer, *Front. Immunol.* 13 (2022) 829451.
- [6] S.S. Wang, W. Liu, D. Ly, H. Xu, L. Qu, L. Zhang, Tumor-infiltrating B cells: their role and application in anti-tumor immunity in lung cancer, *Cell. Mol. Immunol.* 16 (2019) 6–18.
- [7] N.K. Altorki, G.J. Markowitz, D. Gao, J.L. Port, A. Saxena, B. Stiles, T. McGraw, V. Mittal, The lung microenvironment: an important regulator of tumour growth and metastasis, *Nat. Rev. Cancer* 19 (2019) 9–31.
- [8] A. Passaro, J. Brahmer, S. Antonia, T. Mok, S. Peters, Managing resistance to immune checkpoint inhibitors in lung cancer: treatment and novel strategies, *J. Clin. Oncol.* 40 (2022) 598–610.
- [9] M. Duruisseau, M. Esteller, Lung cancer epigenetics: from knowledge to applications, *Semin. Cancer Biol.* 51 (2018) 116–128.
- [10] Y. van der Pol, F. Mouliere, Toward the early detection of cancer by decoding the epigenetic and environmental fingerprints of cell-free DNA, *Cancer Cell* 36 (2019) 350–368.
- [11] W. Dai, J. Zhang, S. Li, F. He, Q. Liu, J. Gong, Z. Yang, Y. Gong, F. Tang, Z. Wang, C. Xie, Protein arginine methylation: an emerging modification in cancer immunity and immunotherapy, *Front. Immunol.* 13 (2022) 865964.
- [12] J. Xu, S. Richard, Cellular pathways influenced by protein arginine methylation: implications for cancer, *Mol. Cell* 81 (2021) 4357–4368.
- [13] Y. Yang, M.T. Bedford, Protein arginine methyltransferases and cancer, *Nat. Rev. Cancer* 13 (2013) 37–50.
- [14] G. Gao, L. Zhang, O.D. Villarreal, W. He, D. Su, E. Bedford, P. Moh, J. Shen, X. Shi, M.T. Bedford, H. Xu, PRMT1 loss sensitizes cells to PRMT5 inhibition, *Nucleic Acids Res.* 47 (2019) 5038–5048.
- [15] X. Yang, Z. Zeng, X. Jie, Y. Wang, J. Han, Z. Zheng, J. Li, H. Liu, X. Dong, G. Wu, S. Xu, Arginine methyltransferase PRMT5 methylates and destabilizes Mxi1 to confer radioresistance in non-small cell lung cancer, *Cancer Lett.* 532 (2022) 215594.
- [16] Y. Kagoya, H. Saijo, Y. Matsunaga, T. Guo, K. Saso, M. Anczurowski, C.H. Wang, K. Sugata, K. Murata, M.O. Butler, C.H. Arrowsmith, N. Hirano, Arginine methylation of FOXP3 is crucial for the suppressive function of regulatory T cells, *J. Autoimmun.* 97 (2019) 10–21.
- [17] Y. Nagai, M.Q. Ji, F. Zhu, Y. Xiao, Y. Tanaka, T. Kambayashi, S. Fujimoto, M.M. Goldberg, H. Zhang, B. Li, T. Ohtani, M.I. Greene, PRMT5 associates with the FOXP3 Homomer and when disabled enhances targeted p185(erbB2/neu) tumor immunotherapy, *Front. Immunol.* 10 (2019) 174.
- [18] M. Inoue, K. Okamoto, A. Terashima, T. Nitta, R. Muro, T. Negishi-Koga, T. Kitamura, T. Nakashima, H. Takayanagi, Arginine methylation controls the strength of γ -family cytokine signaling in T cell maintenance, *Nat. Immunol.* 19 (2018) 1265–1276.
- [19] L. Liu, Q. Hu, Y. Zhang, X. Sun, R. Sun, Z. Ren, Classification molecular subtypes of hepatocellular carcinoma based on PRMT-related genes, *Front. Pharmacol.* 14 (2023) 1145408.
- [20] I.M. Grypari, I. Pappa, T. Papastergiou, V. Zolota, V. Bravou, M. Melachrinou, V. Megalooikonomou, V. Tzelepi, Elucidating the role of PRMTs in prostate cancer using open access databases and a patient cohort dataset, *Histol. Histopathol.* 38 (2023) 287–302.

- [21] D. Zakrzewicz, M. Didiasova, M. Krüger, B.D. Giaimo, T. Borggrefe, M. Mieth, A.C. Hocke, A. Zakrzewicz, L. Schaefer, K.T. Preissner, M. Wygrecka, Protein arginine methyltransferase 5 mediates enolase-1 cell surface trafficking in human lung adenocarcinoma cells, *Biochimica et biophysica acta, Mol. Basis Dis.* 1864 (2018) 1816–1827.
- [22] S. Tomida, T. Takeuchi, Y. Shimada, C. Arima, K. Matsuo, T. Mitsudomi, Y. Yatabe, T. Takahashi, Relapse-related molecular signature in lung adenocarcinomas identifies patients with dismal prognosis, *J. Clin. Oncol.* 27 (2009) 2793–2799.
- [23] H. Okayama, T. Kohno, Y. Ishii, Y. Shimada, K. Shiraishi, R. Iwakawa, K. Furuta, K. Tsuta, T. Shibata, S. Yamamoto, S. Watanabe, H. Sakamoto, K. Kumamoto, S. Takenoshita, N. Gotoh, H. Mizuno, A. Sarai, S. Kawano, R. Yamaguchi, S. Miyano, J. Yokota, Identification of genes upregulated in ALK-positive and EGFR/KRAS/ALK-negative lung adenocarcinomas, *Cancer Res.* 72 (2012) 100–111.
- [24] J. Botling, K. Edlund, M. Lohr, B. Hellwig, L. Holmberg, M. Lambe, A. Berglund, S. Ekman, M. Bergqvist, F. Pontén, A. König, O. Fernandes, M. Karlsson, G. Helenius, C. Karlsson, J. Rahnenführer, J.G. Hengstler, P. Micke, Biomarker discovery in non-small cell lung cancer: integrating gene expression profiling, meta-analysis, and tissue microarray validation, *Clin. Cancer Res.* 19 (2013) 194–204.
- [25] M. Sato, J.E. Larsen, W. Lee, H. Sun, D.S. Shames, M.P. Dalvi, R.D. Ramirez, H. Tang, J.M. DiMaio, B. Gao, Y. Xie, Wistuba II, A.F. Gazdar, J.W. Shay, J. D. Minna, Human lung epithelial cells progressed to malignancy through specific oncogenic manipulations, *Mol. Cancer Res.: MCR* 11 (2013) 638–650.
- [26] H. Tang, G. Xiao, C. Behrens, J. Schiller, J. Allen, C.W. Chow, M. Suraokar, A. Corvalan, J. Mao, M.A. White, Wistuba II, J.D. Minna, Y. Xie, A 12-gene set predicts survival benefits from adjuvant chemotherapy in non-small cell lung cancer patients, *Clin. Cancer Res.* 19 (2013) 1577–1586.
- [27] S.D. Der, J. Sykes, M. Pintilie, C.Q. Zhu, D. Strumpf, N. Liu, I. Jurisica, F.A. Shepherd, M.S. Tsao, Validation of a histology-independent prognostic gene signature for early-stage, non-small-cell lung cancer including stage IA patients, *J. Thorac. Oncol.* 9 (2014) 59–64.
- [28] M.B. Schabath, E.A. Welsh, W.J. Fulp, L. Chen, J.K. Teer, Z.J. Thompson, B.E. Engel, M. Xie, A.E. Berglund, B.C. Creelan, S.J. Antonia, J.E. Gray, S.A. Eschrich, D.T. Chen, W.D. Cress, E.B. Haura, A.A. Beg, Differential association of STK11 and TP53 with KRAS mutation-associated gene expression, proliferation and immune surveillance in lung adenocarcinoma, *Oncogene* 35 (2016) 3209–3216.
- [29] S. Mariathasan, S.J. Turley, D. Nickles, A. Castiglioni, K. Yuen, Y. Wang, E.E. Kadel III, H. Koepfen, J.L. Astarita, R. Cubas, S. Jhunjhunwala, R. Banchereau, Y. Yang, Y. Guan, C. Chalouni, J. Zhai, Y. Şenbabaoglu, S. Santoro, D. Sheinson, J. Hung, J.M. Giltman, A.A. Pierce, K. Mesh, S. Lianoglou, J. Riegler, R.A. D. Carano, P. Eriksson, M. Höglund, L. Somarrriba, D.L. Halligan, M.S. van der Heijden, Y. Loriot, J.E. Rosenberg, L. Fong, I. Mellman, D.S. Chen, M. Green, C. Derleth, G.D. Fine, P.S. Hegde, R. Bourgon, T. Powles, TGF β attenuates tumour response to PD-L1 blockade by contributing to exclusion of T cells, *Nature* 554 (2018) 544–548.
- [30] S. Zhao, Z. Ye, R. Stanton, Misuse of RPKM or TPM normalization when comparing across samples and sequencing protocols, *RNA (New York, N.Y.)* 26 (2020) 903–909.
- [31] H.S. Parker, J.T. Leek, A.V. Favorov, M. Considine, X. Xia, S. Chavan, C.H. Chung, E.J. Fertig, Preserving biological heterogeneity with a permuted surrogate variable analysis for genomics batch correction, *Bioinformatics (Oxford, England)* 30 (2014) 2757–2763.
- [32] M.D. Wilkerson, D.N. Hayes, ConsensusClusterPlus: a class discovery tool with confidence assessments and item tracking, *Bioinformatics (Oxford, England)* 26 (2010) 1572–1573.
- [33] M.E. Ritchie, B. Phipson, D. Wu, Y. Hu, C.W. Law, W. Shi, G.K. Smyth, Limma powers differential expression analyses for RNA-sequencing and microarray studies, *Nucleic Acids Res.* 43 (2015) e47.
- [34] T. Wu, E. Hu, S. Xu, M. Chen, P. Guo, Z. Dai, T. Feng, L. Zhou, W. Tang, L. Zhan, X. Fu, S. Liu, X. Bo, G. Yu, clusterProfiler 4.0: a universal enrichment tool for interpreting omics data, *Innovation (Cambridge (Mass.))* 2 (2021) 100141.
- [35] J. Fu, K. Li, W. Zhang, C. Wan, J. Zhang, P. Jiang, X.S. Liu, Large-scale public data reuse to model immunotherapy response and resistance, *Genome Med.* 12 (2020) 21.
- [36] A. Subramanian, P. Tamayo, V.K. Mootha, S. Mukherjee, B.L. Ebert, G.M. Gillette, A. Paulovich, S.L. Pomeroy, T.R. Golub, E.S. Lander, J.P. Mesirov, Gene set enrichment analysis: a knowledge-based approach for interpreting genome-wide expression profiles, *Proc. Natl. Acad. Sci. U.S.A.* 102 (2005) 15545–15550.
- [37] F. Finotello, Z. Trajanoski, Quantifying tumour-infiltrating immune cells from transcriptomics data, *Cancer Immunol., Immunother.: CII* 67 (2018) 1031–1040.
- [38] K. Yoshihara, M. Shahmoradgoli, E. Martínez, R. Vegesna, H. Kim, W. Torres-García, V. Treviño, H. Shen, P.W. Laird, D.A. Levine, S.L. Carter, G. Getz, K. Stemke-Hale, G.B. Mills, R.G. Verhaak, Inferring tumour purity and stromal and immune cell admixture from expression data, *Nat. Commun.* 4 (2013) 2612.
- [39] Y. Gao, Y. Zhao, J. Zhang, Y. Lu, X. Liu, P. Geng, B. Huang, Y. Zhang, J. Lu, The dual function of PRMT1 in modulating epithelial-mesenchymal transition and cellular senescence in breast cancer cells through regulation of ZEB1, *Sci. Rep.* 6 (2016) 19874.
- [40] N. Cheung, T.K. Fung, B.B. Zeisig, K. Holmes, J.K. Rane, K.A. Mowen, M.G. Finn, B. Lenhard, L.C. Chan, C.W. So, Targeting aberrant epigenetic networks mediated by PRMT1 and KDM4C in acute myeloid leukemia, *Cancer Cell* 29 (2016) 32–48.
- [41] R. Hu, B. Zhou, Z. Chen, S. Chen, N. Chen, L. Shen, H. Xiao, Y. Zheng, PRMT5 inhibition promotes PD-L1 expression and immuno-resistance in lung cancer, *Front. Immunol.* 12 (2021) 722188.
- [42] H.C. Jeong, S.J. Park, J.J. Choi, Y.H. Go, S.K. Hong, O.S. Kwon, J.G. Shin, R.K. Kim, M.O. Lee, S.J. Lee, H.D. Shin, S.H. Moon, H.J. Cha, PRMT8 controls the pluripotency and mesodermal fate of human embryonic stem cells by enhancing the PI3K/AKT/SOX2 Axis, *Stem Cell.* 35 (2017) 2037–2049.
- [43] J. Brahmer, K.L. Reckamp, P. Baas, L. Crinò, W.E. Eberhardt, E. Poddubska, S. Antonia, A. Pluzanski, E.E. Vokes, E. Holgado, D. Waterhouse, N. Ready, J. Gainor, O. Arén Frontera, L. Havel, M. Steins, M.C. Garassino, J.G. Aerts, M. Domine, L. Paz-Ares, M. Reck, C. Baudelet, C.T. Harbison, B. Lestini, D.R. Spigel, Nivolumab versus docetaxel in advanced squamous-cell non-small-cell lung cancer, *N. Engl. J. Med.* 373 (2015) 123–135.
- [44] H. Borghaei, L. Paz-Ares, L. Horn, D.R. Spigel, M. Steins, N.E. Ready, L.Q. Chow, E.E. Vokes, E. Felip, E. Holgado, F. Barlesi, M. Kohlhäuf, O. Arrieta, M. A. Burgio, J. Fayette, H. Lena, E. Poddubska, D.E. Gerber, S.N. Gettinger, C.M. Rudin, N. Rizvi, L. Crinò, G.R. Blumenschein Jr., S.J. Antonia, C. Dorange, C. T. Harbison, F. Graf Finckenstein, J.R. Brahmer, Nivolumab versus docetaxel in advanced nonsquamous non-small-cell lung cancer, *N. Engl. J. Med.* 373 (2015) 1627–1639.
- [45] D.P. Carbone, M. Reck, L. Paz-Ares, B. Creelan, L. Horn, M. Steins, E. Felip, M.M. van den Heuvel, T.E. Ciuleanu, F. Badin, N. Ready, T.J.N. Hiltermann, S. Nair, R. Juergens, S. Peters, E. Minenza, J.M. Wrangle, D. Rodríguez-Abreu, H. Borghaei, G.R. Blumenschein Jr., L.C. Villaruz, L. Havel, J. Krejci, J. Corral Jaime, H. Chang, W.J. Geese, P. Bhagavatheeswaran, A.C. Chen, M.A. Socinski, First-line nivolumab in stage IV or recurrent non-small-cell lung cancer, *N. Engl. J. Med.* 376 (2017) 2415–2426.
- [46] M. Reck, D. Rodríguez-Abreu, A.G. Robinson, R. Hui, T. Csósz, A. Fülöp, M. Gottfried, N. Peled, A. Tafreshi, S. Cuffe, M. O'Brien, S. Rao, K. Hotta, M.A. Leiby, G. M. Lubiniecki, Y. Shentu, R. Rangwala, J.R. Brahmer, Pembrolizumab versus chemotherapy for PD-L1-positive non-small-cell lung cancer, *N. Engl. J. Med.* 375 (2016) 1823–1833.